Thermochimica Acta 616 (2015) 79–86

Contents lists available at ScienceDirect

Thermochimica Acta

journal homepage: www.elsevier.com/locate/tca

Kinetics of the epoxy–thiol click reaction initiated by a tertiary amine: Calorimetric study using monofunctional components

Roi Meizoso Loureiro[a], Tánia Carballeira Amarelo[a], Senen Paz Abuin[a,*], Ezequiel R. Soulé[b], Roberto J.J. Williams[b,**]

[a] Gairesa, Outeiro 1, Lago (Valdoviño), 15551 A Coruña, Spain
[b] Institute of Materials Science and Technology (INTEMA), University of Mar del Plata and National Research Council (CONICET), J. B. Justo 4302, 7600 Mar del Plata, Argentina

ARTICLE INFO

Article history:
Received 3 July 2015
Received in revised form 5 August 2015
Accepted 6 August 2015
Available online 8 August 2015

Keywords:
Click chemistry
DSC
Epoxy–thiol reaction
Induction period
Kinetics
Tertiary amine

ABSTRACT

An analysis of the kinetics of the epoxy–thiol reaction in a model stoichiometric system of monofunctional reagents, 3-mercaptopropionate (BMP) and phenylglycidylether (PGE) is reported. Benzyldimethylamine (BDMA) was employed as initiator in amounts ranging from 0.5 to 2 wt%. These formulations showed a kinetic behavior qualitatively similar to that of commercial adhesives and coatings formulated for a room-temperature cure. Isothermal DSC scans revealed the existence of a relatively long induction period preceding a fast autocatalytic reaction step. Dynamic DSC scans showed that the reaction was shifted to a lower temperature range by increasing the storage period of the initial formulation at 20 °C. This unusual kinetic behavior could be modeled assuming that thiolate anions, slowly generated during the induction period, initiated a fast autocatalytic propagation/proton transfer reaction. The kinetic model included a pseudo-steady state for the initiator concentration and an equilibrium reaction between epoxy and OH groups generated by reaction. A reasonable fitting of isothermal and dynamic DSC runs was achieved in a broad range of temperatures and amine concentrations. In particular, both the length of the induction time and the effect of the storage period were correctly predicted.

1. Introduction

Epoxy formulations are frequently employed as adhesives, coatings or sealants cured at ambient temperature. The diglycidyl ether of bisphenol A (DGEBA) is the most commonly used epoxy monomer. Due to their high reactivity and excellent balance of properties, multifunctional aliphatic amines are the first choice as hardeners for curing at ambient temperature [1]. As the required glass transition temperatures of the products are typically higher than the cure temperature, avoiding arrest of reaction by vitrification needs either external heating or taking advantage of the polymerization heat [1,2]. In fact, it would be desirable to design a formulation exhibiting a large induction period at ambient temperature to provide workability, followed by a fast cure reaction to gain in productivity and as an internal heating source. Formulations using thiols (also called mercaptans) as hardeners can be designed for these purposes. The sector of adhesives, coatings and sealants constitutes one of the major industrial uses of multifunctional thiols [3].

Under appropriate conditions, the reaction of a thiol, RSH, with an epoxy group, R′(O), originates a β-(hydroxy)thioether without secondary reactions, and constitutes a typical example of thiol-click chemistry [3].

$$\text{RSH} + \text{R}'(\text{O}) \rightarrow \text{RS-R}'(\text{OH}) \qquad (1)$$

The epoxy–thiol click reaction is also employed for the synthesis of organic molecules [3], functionalized polymers [4–9], polymer networks [10–12], and two-component healing agents [13–15].

Different catalysts/initiators are employed to produce the epoxy–thiol reaction, the most typical ones being a variety of bases (e.g., hydroxides or tertiary amines). In this case, the reaction proceeds through a typical nucleophilic ring opening reaction. The base generates thiolate anions (RS^-) which give the reaction product by the following propagation/proton transfer reactions [12,16]:

$$\text{RS}^- + \text{R}'(\text{O}) \rightarrow \text{RS-R}'(\text{O})^- \qquad (2)$$

$$\text{RS-R}'(\text{O})^- + \text{RSH} \rightarrow \text{RS}^- + \text{RS-R}'(\text{OH}) \qquad (3)$$

---

* Corresponding author. Tel.: +34 981485478; fax: +34 981485511.
** Corresponding author. Tel.: +54 223 4816600; fax: +54 223 4810046.
E-mail addresses: senen@gairesa.com (S.P. Abuin), williams@fi.mdp.edu.ar (R.J.J. Williams).

http://dx.doi.org/10.1016/j.tca.2015.08.012
0040-6031/© 2015 Elsevier B.V. All rights reserved.

The proton transfer reaction that regenerates the initiator, Eq. (3), proceeds at a much faster rate than the nucleophilic attack of the oxirane ring, Eq. (2). Besides, transfer of a proton from the thiol occurs at a rate that is three orders of magnitude faster compared to the transfer from a secondary alcohol [10,17]. This means that the concentration of alkoxide anions is always very low and explains the absence of epoxy homopolymerization (attack of the alkoxide to an oxirane ring) and the click character of the epoxy–thiol reaction.

The source of thiolate anions is usually ascribed to the acid–base reaction [10,12,16,18]:

$$R''_3N + RSH \leftrightarrow R''_3NH^+ + RS^- \tag{4}$$

The use of strong bases (like LiOH or strong tertiary amines like TBD, MTBD, DBU or DBN) leads to a fast generation of thiolate anions. In some cases, it is necessary to cool to 0 °C to control the reaction rate [5], or to use a complex of the strong base that is decomposed by UV irradiation [11,19].

Although, strong bases are normally used for the synthesis of organic molecules or functionalized polymers, they cannot be used for formulating adhesives or coatings for industrial applications. These formulations require a workability period (induction period) at room temperature where the viscosity remains practically constant, followed by a period where the reaction takes place at a relatively fast rate. Formulators use initiating systems exhibiting the desired behavior at the temperature of application. Typical initiators for this purpose are based on conventional tertiary amines of low/medium basicity. In these cases, the acid-base equilibrium represented by Eq. (4) is shifted to the left and the initiation mechanism involves an alternative route.

The focus of this study was placed on the analysis of the kinetics of an epoxy–thiol reaction exhibiting a significant induction period at room temperature. A model system consisting of stoichiometric amounts of a monofunctional epoxy and a monofunctional thiol was selected together with variable amounts of benzyldimethylamine (BDMA) as initiator. The reaction kinetics was analyzed employing differential scanning calorimetry (DSC) in both isothermal and dynamic modes. A mechanistic model was build-up that provided a reasonable fitting of the unusual kinetic behavior of this reaction.

2. Experimental

2.1. Materials

Formulations were prepared using stoichiometric amounts of butyl 3-mercaptopropionate (BMP, Sigma–Aldrich, 98%) and phenylglycidylether (PGE, Sigma–Aldrich, 99%). Benzyldimethylamine (BDMA, Sigma–Aldrich, 99%) was used as initiator in amounts equal to 0.5, 1, 1.4 or 2 wt% (expressed with respect to the total mass). The effect of adding a secondary alcohol (MPOH, 4-methyl-2-pentanol, Sigma–Aldrich, 98%) to the initial formulation, was analyzed. Chemical structures of these compounds are shown in Fig. 1.

2.2. Size exclusion chromatography

A formulation with 1.4 wt% BDMA was reacted at 30 °C. Samples taken at different times were dissolved in THF (approximate concentration equal to 2000 ppm), treated in an ultrasonic bath for 5 min at room temperature, filtered and injected (150 μL) in a size exclusion chromatograph (HPLC 1515 with Styragel HR columns and refractive index detector 2414, Waters). Chromatograms were taken employing THF as solvent at a flow rate of 1 mL/min, under isocratic conditions, at 30 °C (in both oven and detector). The calibration of the equipment was made with polystyrene standards in a range of molecular weights between 162 and 3470 Da and a DGEBA standard ($n = 0$) with a molecular weight of 340 Da.

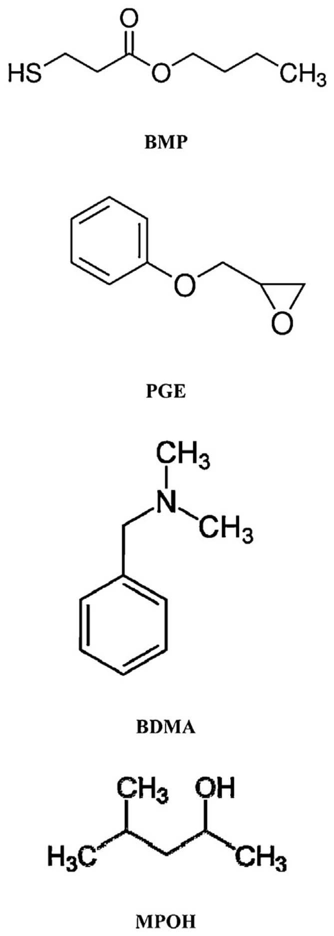

Fig. 1. Chemical structures of BMP, PGE, BDMA and MPOH.

2.3. Near-infrared spectroscopy

The reaction of a formulation with 1.4 wt% BDMA at 20 °C, was followed by Fourier-transformed infrared spectroscopy (FTIR) in the 4000–7000 cm^{-1} near infrared range. A Perkin Elmer Spectrum Two device with a KBr cell was employed. Spectra (10 scans) were obtained every 5 min with a resolution of 4 cm^{-1}.

2.4. Differential scanning calorimetry

Formulations containing from 0.5 to 2 wt% BDMA were reacted in a differential scanning calorimeter (DSC 8500, Perkin Elmer), equipped with an intracooler. Samples of approximately 5 mg, placed in closed aluminum pans with a hole in the lid, were analyzed under nitrogen atmosphere. Dynamic scans were performed at 10 °C/min from −10 to 220 °C, and isothermal scans at 30, 40, 50, 60 and 70 °C. The effect of a previous storage period at 20 °C was investigated for formulations with the three components (BMP, PGE and BDMA) and four components (BMP, PGE, BDMA and MPOH). In the last case, MPOH was added in an amount simulating 40% conversion (relative amount of secondary hydroxyls generated at this conversion). Besides, the effect of the storage period was analyzed by mixing two of the three components, keeping the mixture at 20 °C for a pre-determined period, adding the third component and carrying out a dynamic DSC scan.

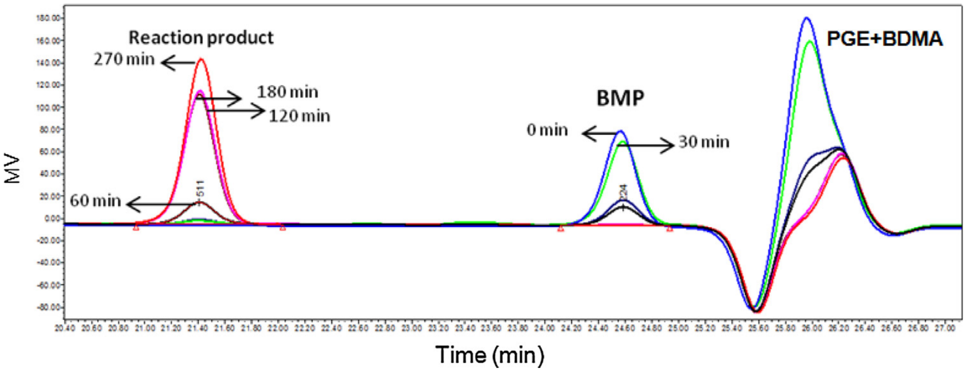

Fig. 2. Size exclusion chromatograms taken at different times for the reaction at 30 °C initiated by 1.4 wt% BDMA.

3. Results and discussion

3.1. Isothermal reaction

Size exclusion chromatography was employed to confirm the click character of the reaction. A set of chromatograms taken at different times during reaction at 30 °C for a formulation containing 1.4 wt% BDMA, is shown in Fig. 2. BMP and the reaction product gave clear well-separated peaks while PGE and BDMA eluted at similar times at the end of the chromatogram, in a region disturbed by the injection peak.

The area of the peak of BMP decreased while the area of the peak of the reaction product increased continuously. At the end of reaction, the signal of BMP disappeared completely while the signal of the reaction product remained constant. This test confirmed that only one main reaction product was generated. The evolution of the areas under both peaks is shown in Fig. 3.

During the first 2 h, a very low increase in conversion was observed. After this induction period, the reaction took place at a fast rate following an autocatalytic mechanism Therefore, BDMA simulates correctly the induction period needed in commercial formulations for workability purposes as well as the fast cure rate expected after the induction period.

The occurrence of the epoxy–thiol click reaction was further confirmed by FT-NIR. The reaction of the formulation with 1.4 wt% BDMA was followed at 20 °C during 18 h. The following results were recorded: disappearance of characteristic bands of epoxy groups (at 4530 cm^{-1}), and of thiol groups (at 5051 cm^{-1}); appearance and increase in intensity of a band at about 4800 cm^{-1}, assigned to the OH groups generated during reaction.

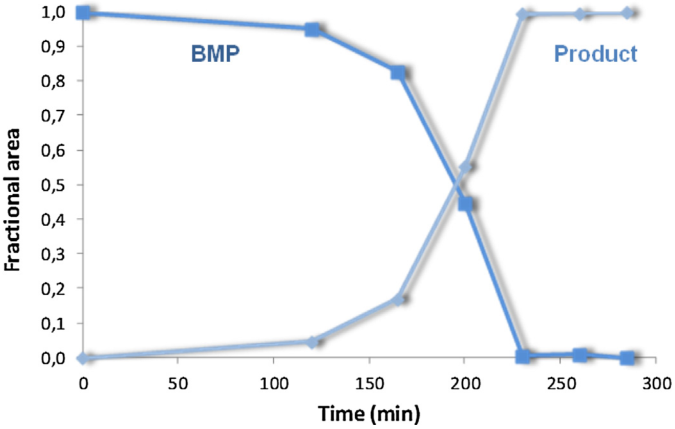

Fig. 3. Evolution of the concentrations of BMP and the reaction product for a reaction carried out at 30 °C, initiated with 1.4 wt% BDMA.

Although SEC and FT-NIR could be used to follow the kinetics, DSC was a more reliable technique due to the precise control of temperature, particularly under fast-rate conditions, as well as the possibility to employ temperature ramps. Therefore, DSC was used to analyze the kinetics of the epoxy–thiol click reaction.

Isothermal DSC scans for formulations containing 1.4 wt% BDMA reacted at different temperatures, are shown in Fig. 4. Isothermal DSC scans for formulations with different BDMA amounts, reacted at 40 °C, are shown in Fig. 5. In every case, the kinetics was characterized by a large induction period followed by a relatively fast reaction rate exhibiting an autocatalytic behavior.

3.2. Total reaction heat

Dynamic DSC runs were performed for formulations containing 1.4 wt% BDMA after different storage periods at 20 °C (Fig. 6).

The reaction peak was shifted to a lower temperature range by increasing the storage period of the initial formulation. Table 1 shows the total reaction heats and the location of the maximum temperature of the reaction peak. The total reaction heat remained almost constant during the first 180 min meaning that the increase in conversion was undetectable by calorimetry during this period. However, a precursor was generated that enabled the starting of the reaction at lower temperatures in subsequent DSC scans.

The average reaction heat recorded for samples stored up to 180 min was 408.6 J/g or 129.5 kJ/mol. This value is close to a set of values recently reported in the literature for the epoxy–thiol reaction initiated by different tertiary amines, located in the range comprised between 120 and 128 kJ/mol [12]. Other values reported in the literature for the same reaction are 117 kJ/mol [18], and 132.2 kJ/mol (calculated from Ref. [14] using reported values per unit mass).

Table 1
Effect of the storage period at 20 °C on the total reaction heat and the maximum temperature of the reaction peak observed in a subsequent DSC run at 10 °C/min, for a formulation containing stoichiometric amounts of BMP and PGE with 1.4 wt% BDMA.

Storage period (min)	Reaction heat (J/g)	Peak temperature (°C)
0	400.7	134
30	413.0	132.7
60	419.8	129.0
120	409.1	119.9
180	400.5	96.1
270	20.5	65.8

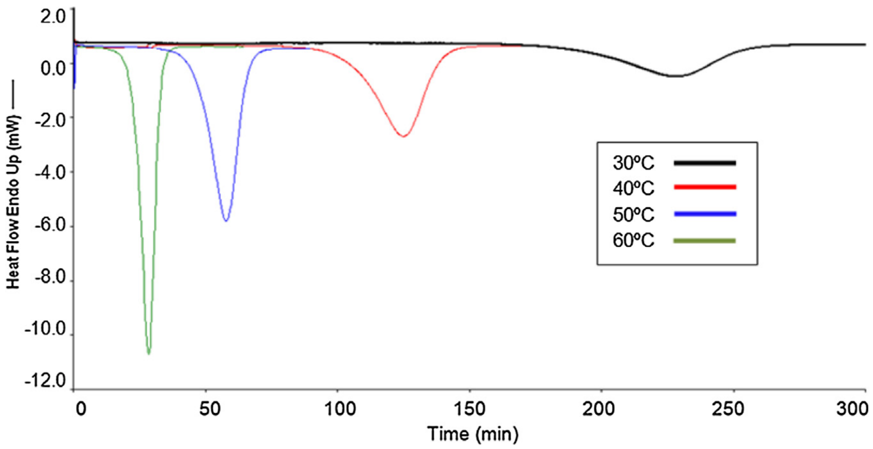

Fig. 4. Isothermal DSC scans for formulations containing 1.4 wt% BDMA reacted at different temperatures.

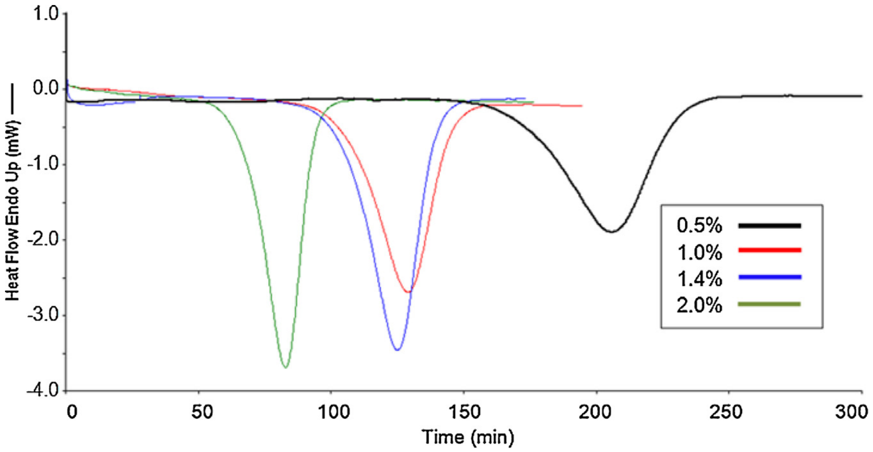

Fig. 5. Isothermal DSC scans for formulations containing different BDMA amounts, reacted at 40 °C.

3.3. *Analysis of reactions taking place during the induction period*

Mixtures of two of the three components (BMP, PGE and BDMA) in the same proportions as in the ternary blend were stored for different times at 20 °C. Then the third component was added and a DSC scan was carried out immediately. The storage of BMP together with PGE before the addition of BDMA did not produce any significant effect. The same happened when BMP and BDMA were stored together before the addition of PGE. However, the situation was different when PGE and BDMA were stored together before the addition of BMP. Results are shown in Table 2.

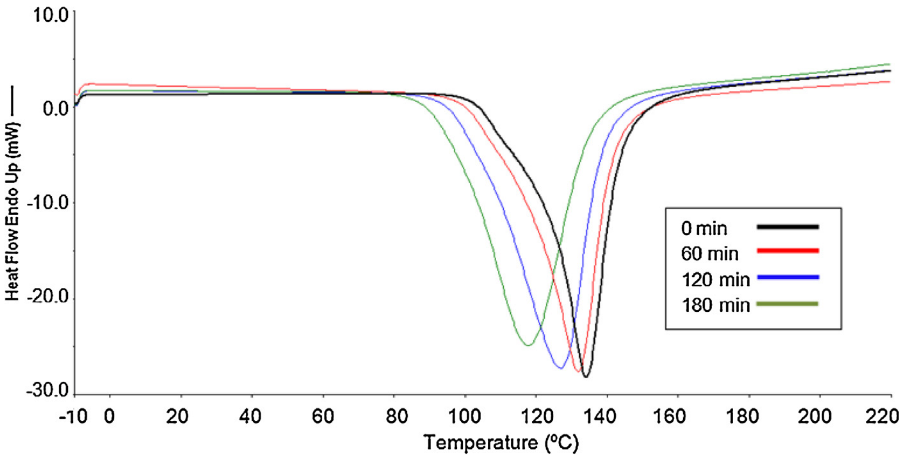

Fig. 6. Dynamic DSC runs for formulations containing 1.4 wt% BDMA after different storage periods at 20 °C.

Table 2

Total reaction heat and the maximum temperature of the reaction peak for a formulation containing PGE and BDMA in similar proportions as in the ternary mixture that was stored at 20 °C for different times, followed by addition of the stoichiometric amount of BMP before carrying out the DSC scan.

Storage period (h)	Reaction heat (J/g)	Peak temperature (°C)
0	400.7	134
24	327.4	78.0
48	268.1	59.0
96	26.7	52.8

The homopolymerization of PGE took place in the presence of BDMA during the storage period at 20 °C. This was also confirmed by the appearance of high molar mass peaks in SEC chromatograms (results not shown). This reaction is initiated by the attack of a tertiary amine to an activated oxirane ring:

$$R''_3N + R'(O)\ldots HX \rightarrow R''_3N^{+}\text{-}R'(O)^{-} + HX \tag{5}$$

The presence of a protic compound, HX, is necessary to produce the reaction. Impurities or absorbed humidity can be responsible for the initiation while OH groups generated in termination reactions can accelerate the rate at which the zwitterion is generated [20].

In the presence of BMP, a proton transfer reaction takes place generating thiolate anions:

$$R''_3N^{+}\text{-}R'(O)^{-} + RSH \rightarrow R''_3N^{+}\text{-}R'(OH) + RS^{-} \tag{6}$$

Due to this reaction, the storage of the three components produced a faster initiation of the epoxy–thiol reaction observed in subsequent DSC scans.

3.4. *Effect of adding a secondary alcohol*

The effect of adding a secondary alcohol (MPOH) to the initial formulation, in an amount equivalent to a 40% conversion, was analyzed. Results of DSC scans carried out after different storage periods are shown in Table 3.

Table 1 showed that there was no significant advance in conversion for the sample without MPOH after 180 min. The induction period was reduced to about 120 min for the formulation with MPOH. The rate at which the precursor was generated was also faster in the presence of MPOH as revealed by the shift of the reaction peak to lower temperatures at the same storage times. However, the effect was not as significant as expected implying that the activation effect of MPOH was not equivalent to the activation produced by the reaction product. To keep the analysis as simple as possible, the kinetic scheme was limited to formulations without MPOH.

Table 3

Effect of the storage period at 20 °C on the total reaction heat and the maximum temperature of the reaction peak observed in a subsequent DSC run at 10 °C/min, for a formulation containing MPOH in an amount simulating a 40% conversion.

Storage period (min)	Reaction heat (J/g)	Peak temperature (°C)
0	379.8	118.9
20	369.9	112.0
40	374.1	108.6
60	370.8	102.4
90	369.4	95.5
120	359.0	85.8
150	309.8	72.8

3.5. *Kinetic scheme*

Based on the previous experimental results, different kinetic schemes were proposed attempting to fit the unusual behavior of this system (long induction periods followed by a fast autocatalytic reaction). Of all tested models, the one described in what follows provided a reasonable fitting of kinetic curves.

During the initiation period, we assume that the epoxy–thiol reaction takes place at a slow rate by an alternative mechanism than the one involving the thiolate anion:

$$RSH + R'(O) + R''_3N \rightarrow RS\text{-}R'(OH) + R''_3N \tag{7}$$

A complex is then formed between the oxirane ring and the reaction product:

$$R'(O) + RS\text{-}R'(OH) \leftrightarrow R'(O)\ldots(OH)R'\text{-}SR \tag{8}$$

The activation of the oxirane ring enables the generation of the zwitterion by the slow nucleophilic reaction:

$$R''_3N + R'(O)\ldots(OH)R'\text{-}SR \rightarrow R''_3N^{+}\text{-}R'(O)^{-} + RS\text{-}R'(OH) \tag{9}$$

A fast proton transfer reaction takes place generating the thiolate anion:

$$R''_3N^{+}\text{-}R'(O)^{-} + RSH \rightarrow R''_3N^{+}\text{-}R'(OH) + RS^{-} \tag{10}$$

The thiolate anion attacks the activated epoxy groups:

$$RS^{-} + R'(O)\ldots(OH)R'\text{-}SR \rightarrow RS\text{-}R'(O)^{-} + RS\text{-}R'(OH) \tag{11}$$

A fast proton transfer reaction generates the product and regenerates the initiator:

$$RS\text{-}R'(O)^{-} + RSH \rightarrow RS^{-} + RS\text{-}R'(OH) \tag{12}$$

The concentration of the thiolate anion is limited by a termination reaction:

$$RS^{-} + R''_3N^{+}\text{-}R'(OH) \rightarrow RS\text{-}R'(OH) + R''_3N \tag{13}$$

Kinetic equations are written using the following notation:

$E = R'(O)$ (free epoxy groups)
$P = RS\text{-}R'(OH)$ (reaction product)
$E\text{–}P = R'(O)\ldots(OH)R'\text{-}SR$ (complex of an epoxy group with the reaction product)
$T = RSH$ (thiol)
$I = S^{-}$ (thiolate anion)
$A = R''_3N$ (tertiary amine)
$N^{+} = R''_3N^{+}\text{-}R'(OH)$ (cation)

The following assumptions are made:

(a) There is an equilibrium between E and E–P expressed by:

$$(E-P) \leftrightarrow K(E)(P) \tag{14}$$

(b) There is a pseudo-steady state for the concentration of the thiolate anion derived by equating initiation and termination rates.

The rate at which thiolate anion is generated is controlled by Eq. (9). Proton transfer (Eq. (10)) takes place at a much faster rate. Therefore, the initiation rate is given by:

$$R_i = k_i(A)(E-P) \tag{15}$$

The termination rate is given by:

$$R_t = k_t(I)(N^{+}) = k_t(I)^2 \tag{16}$$

The condition $(I) = (N^{+})$ is necessary to equilibrate negative and positive charges. The pseudo-steady state concentration of initiator arises by equating R_i and R_t. This gives:

$$(I) = \left(\frac{k_i}{k_t}\right)^{1/2}(A)^{1/2}(E-P)^{1/2} \tag{17}$$

(c) The fraction of S atoms present in the initiator is negligible with respect to the fractions present in the unreacted thiol, the reaction product and the complex of the reaction product with epoxy groups. The following balance may be written:

$$(T)_0 = (T) + (P) + (E-P) \tag{18}$$

(d) The fraction of epoxy groups present in N^+ is negligible with respect to the fractions of unreacted epoxy groups and those present in the reaction product and in the complex with unreacted epoxies. This gives:

$$(E)_0 = (E) + (P) + 2(E-P) \tag{19}$$

Besides,

$$(E)_0 = (T)_0 \tag{20}$$

(e) The fraction of nitrogen atoms present in N^+ is negligible with respect to the fraction present as free amine:

$$(A) = (A)_0 \tag{21}$$

The conversion of epoxy groups is given by:

$$x = \frac{[(P) + (E-P)]}{(E)_0} \tag{22}$$

Neglecting the generation of reaction product by the termination reaction, Eq. (13), the two reactions that consume epoxy groups are Eq. (7) (significant to determine the extent of the induction period), and the propagation reaction, Eq. (11) (main reaction after the induction period). The following rate equation may be written:

$$(E)_0 \frac{dx}{dt} = k_0(A)_0(E)(T) + k_p(I)(E-P) \tag{23}$$

From Eqs. (18) to (20) and (22),

$$(T) = (1-x)(E)_0 \tag{24}$$

Using Eqs. (17), (21) and (24), the rate equation may be finally written as:

$$dx/dt = k_0(A)_0(E)(1-x) + k_1(A)_0^{1/2}(E-P)^{3/2}/(E)_0 \tag{25}$$

With $k_1 = k_p(k_i/k_t)^{1/2}$.

Functions giving the concentrations of (E) and (E − P) may be obtained from Eqs. (14), (18)–(20) and (22):

$$(E) = \frac{F(x)}{K} \tag{26}$$

$$(E-P) = \frac{xF(x)(E)_0}{[1+F(x)]} \tag{27}$$

where

$$F(x) = \{[G(x)^2 + K(E)_0(1-x)]^{1/2} - G(x)\} \tag{28}$$

$$G(x) = \frac{[1+K(E)_0(2x-1)]}{2} \tag{29}$$

The fitting of the complex kinetic behavior required two rate constants, $k_0(T)$ and $k_1(T)$, and an equilibrium constant, $K(T)$.

3.6. Fitting of kinetic results

A simultaneous fitting of 16 isothermal DSC runs (four amine concentrations at four different temperatures) and five dynamic runs (five different storage times at 20 °C and a single amine concentration), was performed. This comprises a temperature range extending from 20 °C to about 170 °C and induction periods extending up to about 170 min. A minimum of the following function was searched:

$$\min\left\{\sum (x-x_i)^2(\text{iso}) + w\sum (x-x_i)^2(\text{dyn})\right\} \tag{30}$$

where x represents calculated conversions and x_i experimental conversions (obtained from fractional areas of the reaction peaks). A weight factor $w = 5$ was used to balance the fact that five dynamic runs were used with respect to 16 isothermal runs. Concentrations were expressed in mol L^{-1} using molar masses and densities of every compound.

The minimum was searched using Scilab software and quasi-Newton algorithm. The following set of kinetic and equilibrium functions was found (T is expressed in Kelvin):

$$k_0\ \ (\mathrm{L^2\,mol^{-2}\,min^{-1}}) = 8.957 \times 10^5 \exp\left(\frac{-6946}{T}\right) \tag{31}$$

$$k_1\ \ (\mathrm{L\,mol^{-1}\,min^{-1}}) = 8.375 \times 10^{12} \exp\left(\frac{-10586}{T}\right) \tag{32}$$

$$K\ \ (\mathrm{L\,mol^{-1}}) = 2.23 \times 10^{-10} \exp\left(\frac{7738}{T}\right) \tag{33}$$

The equilibrium constant decreases with temperature as expected for the formation of a complex involving H-bonds.

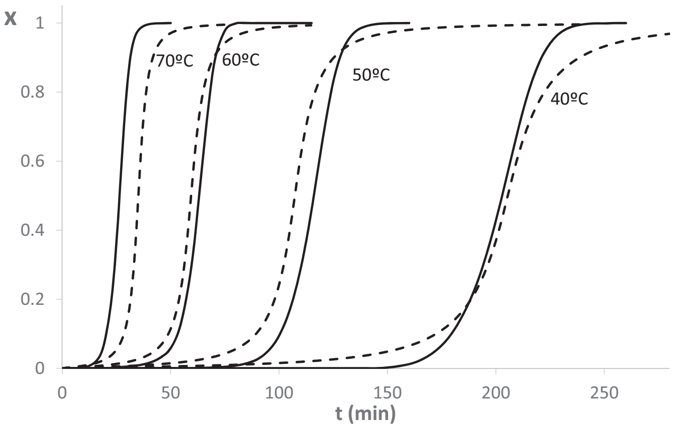

Fig. 7. Conversion vs. time curves obtained from isothermal DSC runs for formulations containing 0.5 wt% BDMA, at 40, 50, 60 and 70 °C. Continuous curves represent experimental values while dashed curves are model simulations.

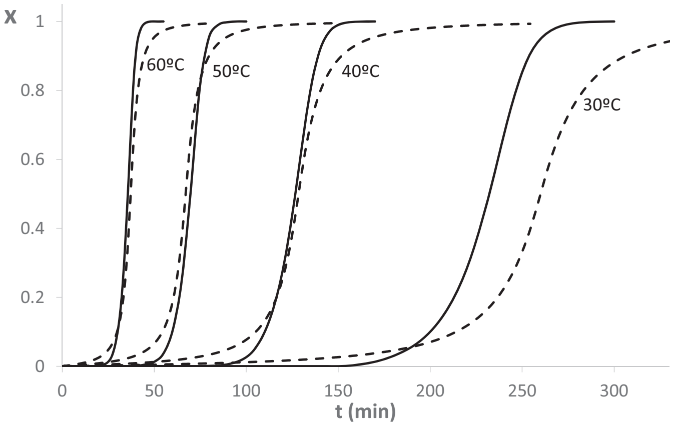

Fig. 8. Conversion vs. time curves obtained from isothermal DSC runs for formulations containing 1 wt% BDMA, at 30, 40, 50 and 60 °C. Continuous curves represent experimental values while dashed curves are model simulations.

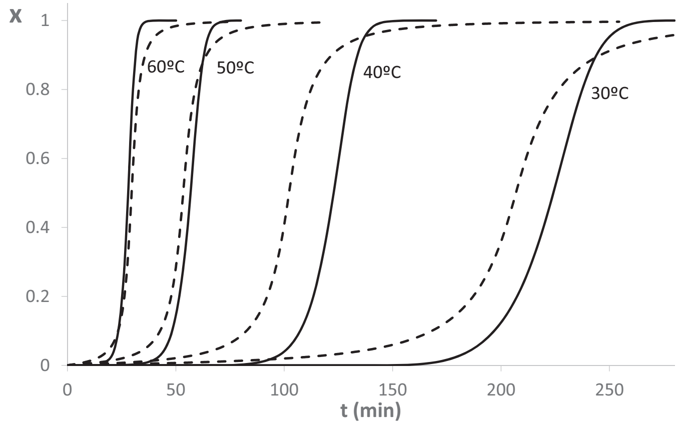

Fig. 9. Conversion vs. time curves obtained from isothermal DSC runs for formulations containing 1.4 wt% BDMA, at 30, 40, 50 and 60 °C. Continuous curves represent experimental values while dashed curves are model simulations.

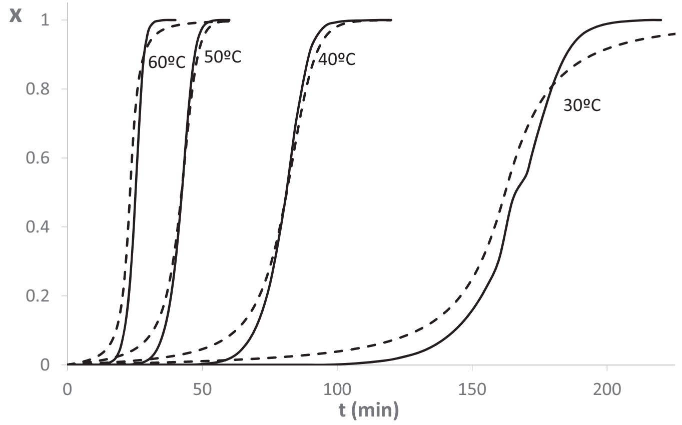

Fig. 10. Conversion vs. time curves obtained from isothermal DSC runs for formulations containing 2 wt% BDMA, at 30, 40, 50 and 60 °C. Continuous curves represent experimental values while dashed curves are model simulations.

Figs. 7–10 show the optimum fitting of isothermal DSC runs and Fig. 11 shows the fitting of dynamic DSC runs.

The fitting was considered reasonable taking into account the broad temperature and induction time ranges that were covered. Main deviations are the rather smooth increase and end of DSC curves predicted by the model compared to the sharp initiation and end observed experimentally. Independently of the lack of an exact fitting, the simple kinetic model provides a reasonable prediction of the length of the induction period, the fast autocatalytic rate following the induction period and the effect of a previous storage at 20 °C.

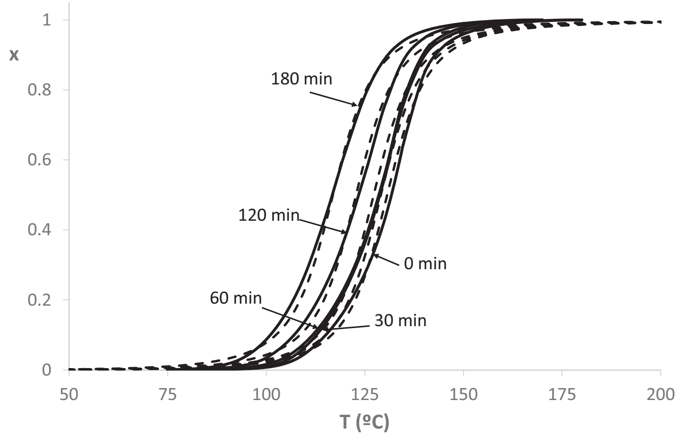

Fig. 11. Conversion vs. temperature curves obtained from dynamic DSC runs for a formulation containing 1.4 wt% BDMA, at different storage periods at 20 °C (0, 30, 60, 120 and 180 min). Continuous curves represent experimental values while dashed curves are model simulations (2nd and 3rd curves are very close).

4. Conclusions

An analysis of the kinetics of the epoxy–thiol reaction in a model system of monofunctional reagents, in the presence of BDMA as initiator, was reported. The significance of this system is related to the fact that an induction period preceded a fast reaction step, simulating the behavior of commercial adhesives and coatings formulated for a room-temperature cure. This unusual kinetic behavior could be modeled assuming that thiolate anions, slowly generated during the induction period, initiated a fast autocatalytic propagation/proton transfer reaction. The kinetic model included a pseudo-steady state for the initiator concentration and an equilibrium reaction between epoxy and OH groups generated by reaction. A reasonable fitting of isothermal and dynamic DSC runs was achieved in a broad range of temperatures and amine concentrations. In particular, both the length of the induction time and the effect of a storage period before reaction were correctly predicted.

Acknowledgments

E.R. Soulé and R.J.J. Williams acknowledge the financial support of the University of Mar del Plata, ING/438/15, the National Research Council (CONICET), PIP100125 and the National Agency for the Promotion of Science and Technology (ANPCyT), PICT10-1008, Argentina.

References

[1] S. Paz Abuín, Epoxy adhesives: a view of the present and the future, in: J.P. Pascault, R.J.J. Williams (Eds.), Epoxy Polymers: New Materials and Innovations, Wiley-VCH, Weinheim, 2010, pp. 215–234.
[2] C. Esposito Corcione, F. Freuli, M. Frigione, Cold-cure structural epoxy resins: analysis of the curing reaction as a function of curing time and thickness, Materials 7 (2014) 6832–6842.
[3] C.E. Hoyle, A.B. Lowe, C.N. Bowman, Thiol-click chemistry: a multifaceted toolbox for small molecule and polymer synthesis, Chem. Soc. Rev. 39 (2010) 1355–1387.
[4] S. De, C. Stelzer, A. Khan, A general synthetic strategy to prepare poly(ethyleneglycol)-based multifunctional copolymers, Polym. Chem. 3 (2012) 2342–2345.
[5] A. Brändle, A. Khan, Thiol–epoxy “click” polymerization: efficient construction of reactive and functional polymers, Polym. Chem. 3 (2012) 3224–3227.
[6] S. De, A. Khan, Efficient synthesis of multifunctional polymers via thiol–epoxy click chemistry, Chem. Commun. 48 (2012) 3130–3132.
[7] N. Cengiz, J. Rao, A. Sanyal, A. Khan, Designing functionalizable hydrogels through thiol–epoxy coupling chemistry, Chem. Commun. 49 (2013) 11191–11193.
[8] I. Gadwal, A. Khan, Protecting-group-free synthesis of chain-end multifunctional polymers by combining ATRP with thiol–epoxy “click” chemistry, Polym. Chem. 4 (2013) 2440–2444.
[9] S. Binder, I. Gadwal, A. Bielmann, A. Khan, Thiol–epoxy polymerization via an AB monomer: synthetic access to high molecular weight poly(β-hydroxythio-ether)s, J. Polym. Sci. A: Polym. Chem. 52 (2014) 2040–2046.
[10] J.A. Carioscia, J.W. Stansbury, C.N. Bowman, Evaluation and control of thiol–ene/thiol–epoxy hybrid networks, Polymer 48 (2007) 1526–1532.
[11] Y. Jian, Y. He, Y. Sun, H. Yang, W. Yang, J. Nie, Thiol–epoxy/thiol–acrylate hybrid materials synthesized by photopolymerization, J. Mater. Chem. C 1 (2013) 4481–4489.
[12] D. Guzmán, X. Ramis, X. Fernández-Francos, A. Serra, New catalysts for diglycidyl ether of bisphenol A curing based on thiol–epoxy click reaction, Eur. Polym. J. 59 (2014) 377–386.
[13] Y.C. Yuan, M.Z. Rong, M.Q. Zhang, J. Chen, G.C. Yang, X.M. Li, Self-healing polymeric materials using epoxy/mercaptan as the healant, Macromolecules 41 (2008) 5197–5202.

[14] Y.C. Yuan, M.Z. Rong, M.Q. Zhang, G.C. Yang, Study of factors related to performance improvement of self-healing epoxy based on dual encapsulated healant, Polymer 50 (2009) 5771–5781.
[15] Y.C. Yuan, M.Z. Rong, M.Q. Zhang, G.C. Yang, J.Q. Zhao, Self-healing of fatigue crack in epoxy materials with epoxy/mercaptan system, eXPRESS Polym. Lett. 5 (2011) 47–59.
[16] I. Gadwal, S. Binder, M.C. Stuparu, A. Khan, Dual-reactive hyperbranched polymer synthesis through proton transfer polymerization of thiol and epoxide groups, Macromolecules 47 (2014) 5070–5080.
[17] A. Steitwieser Jr., Solvolytic displacement reactions at saturated carbon atoms, Chem. Rev. 56 (1956) 571–752.
[18] T. Kamon, Isothermal DSC study on curing of epoxy resins with polymercaptans, Kobun. Robun. 43 (1986) 563–571.
[19] K. Dietliker, R. Husler, J.L. Birbaum, S. Ilg, S. Villeneuve, K. Studer, T. Jung, J. Benkhoff, H. Kura, A. Matsumoto, H. Oda, Advances in photoinitiators – opening up new applications for radiation curing, Prog. Org. Coat. 58 (2007) 146–157.
[20] I.E. Dell'Erba, R.J.J. Williams, Homopolymerization of epoxy monomers initiated by 4-(dimethylamino)pyridine, Polym. Eng. Sci. 46 (2006) 351–359.